2D multilayered perovskites and 2D/3D bilayers for stable solar cells

Jacky Even, Siraj Sidhik, Mikael Kepenekian, Boubacar Traoré, Claudine Katan, Mercouri Kanatzidis, Aditya Mohite

2D multilayered perovskites and 2D/3D bilayers for stable solar cells

Jacky Even*[a], Siraj Sidhik[b,c], Mikael Kepenekian[d], Boubacar Traoré[d], Claudine Katan[d], Mercouri G. Kanatzidis[e], Aditya D. Mohite[b,c]

[a]Univ Rennes, INSA Rennes, CNRS, Institut FOTON − UMR 6082, F-35000 Rennes, France; [b]Department of Material Science and Nanoengineering, Rice University, Houston, TX 77005, USA; [c]Department of Chemical and Biomolecular Engineering, Rice University, Houston, TX 77005, USA; [d]Univ Rennes, ENSCR, CNRS, ISCR − UMR 6226, F-35000 Rennes, France; [e]Department of Chemistry and Department of Materials Science and Engineering, Northwestern University, Evanston, IL 60208, USA

ABSTRACT

The contribution focuses on a theoretical analysis of 2D multilayered halide perovskites, and their interfaces with 3D perovskites. At present, perovskite materials are mixed with each other in complex alloys and heterostructures, including 2D/3D compositions, combined with additives or protecting layers to improve their stability as well as assembled with carrier selective layers. The specificities of the mechanical properties of halide perovskites by comparison to classical semiconductors and the role played by large cations in the interlayer of the 2D perovskite are discussed.

Keywords: Density functional theory, perovskite, heterostructure, solar cell, elasticity

1. INTRODUCTION

The great success of halide perovskites in the design of solar cells with record efficiencies comes from the use of 3D halide perovskite alloys such as $Cs_{0.05}(MA_{0.10}FA_{0.85})Pb(I_{0.90}Br_{0.10})_3$ [1]. In those materials, a mixture of small organic (FA is formamidinium and MA methylammonium) and inorganic (Cs^+) cations is used to avoid the structural transformations of pure $CsPbI_3$ and $FAPbI_3$ into related non-perovskite yellow phases. In recent years, the blending of 2D perovskite phases with 3D perovskite bulk material to form 2D/3D heterostructures has become one of the prevailing strategies to afford perovskite active materials with superior stability and efficiency both in the prospect of perovskite-based light emitting diodes (PeLEDs) [2] and perovskite-based photovoltaics (PePVs) [3-5]. Whilst the diversity of the 3D perovskite composition is rather limited, that of 2D is almost unlimited thanks to the insertion of more or less bulky organic monovalent or divalent cations. The molecules (more rarely atomic species) template mono- (n=1) or multi-layered (n>1) structures having quantum wells composed of n-layers of corner-sharing metal-halide octahedra. The layers separated by the organic barrier can be piled on top of each other with or without in-plane shifts, for instance either eclipsed, also known as Dion-Jacobson (DJ) phase, or staggered, as in the most frequently reported Ruddlesden-Popper (RP) phase. Besides, phase pure multi-layered perovskites (e.g. n=4) on their own are also good candidates for PePV with power conversion efficiencies above 15%, which can be further enhanced thanks to beneficial light-induced activation of interlayer charge transport when the superlattice packing is favourable [6]. Given this versatility, concept and tools that guide the choice of 2D and 3D compositions are crucial.

Recently, we introduced and adapted the concept of lattice mismatch coming from semiconductor heterostructures to halide perovskites [7]. The concept is using experimental room temperature data for bulk materials to compute the lattice mismatch and relies on the idea that built-up strain shall be minimized in order to obtain stabilized heterointerfaces, because the elastic free energy has a quadratic variation as a function of the lattice mismatch. It was shown additionally that flexible molecules in the barrier may limit to a certain extent the accumulation of strain energy in the heterostructure. This concept allowed a better understanding of the known multi-layered perovskite materials.

In the present contribution, we recall the specificities of the mechanical properties of halide perovskites by comparison to classical semiconductors. Then, we consider the effect of strains on the electronic levels of halide perovskites. After a discussion on the challenges raised by mixed cations halide perovskite alloys for computational description, we, finally,

explore the energy level alignments of 2D and 3D moieties in 2D/3D heterostructures in the context of engineering of complex halide perovskite heterostructures.

*jacky.even@insa-rennes.fr

2. IMPORTANCE OF LATTICE STRAIN IN THE FORMATION OF 2D/3D PEROVSKITE HETEROSTRUCTURES

2.1 Lattice mismatch in heterostructures of classical semiconductors.

For the epitaxial growth of coherent semiconductor heterostructures, an important parameter to be considered is the in-plane lattice mismatch between the substrate and the epilayer (Figure 1). In-plane compressive (tensile) strain is partially compensated by an out-of-plane tensile (compressive) strain, which depends in classical semiconductors on a ratio of elastic constants. The strain field usually corresponding to bond stretching or compression at the microscopic level. For moderate lattice mismatches (<1%) in classical III-V semiconductors, 2D quantum well-like structures can be grown up to a thickness of a few nm before turning into the formation of 0D islands [8]. This formation can be observed at smaller critical thicknesses by increasing the initial lattice mismatch or changing the substrate orientation. For large lattice mismatches, the growth of coherent interfaces is impossible, and extended defects (dislocations) are observed.

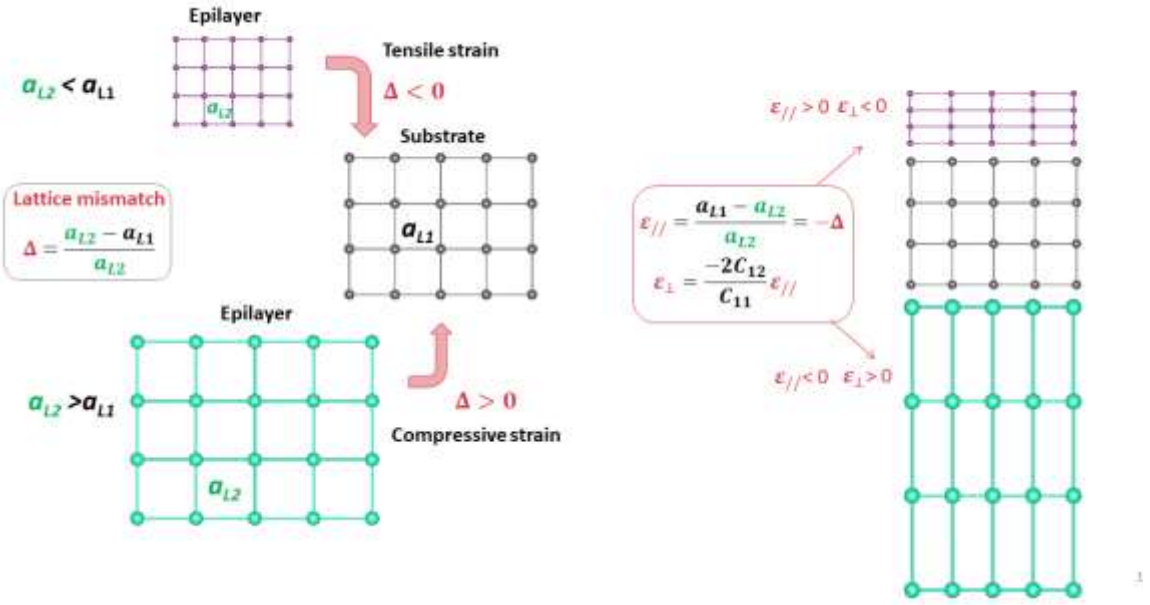

Figure 1. Schematic representation of the anisotropic tensile and compressive in-plane (parallel) strain components for a coherent simple epilayer deposited on a substrate with a (001) orientation. The resulting out-of-plane (perpendicular) components are represented.

For small lattice mismatches on a (001) substrate, the minimization of the elastic energy of the 2D epitaxial layer leads to the relation between in-plane and out-of-plane strain components: $\varepsilon_{\perp} = \frac{-2C_{12}}{C_{11}} \varepsilon_{//}$ [7].

2.2 Mechanical properties of bulk halide perovskites

Halide perovskites are ultrasoft semiconductors by comparison to classical semiconductors [9]. They especially exhibit very small shear elastic moduli. At the microscopic level, these unusual features are basically explained by the very strong anharmonicity of the lattice [10,11], and in-plane and out-of-plane octahedra tilting modes leading to additional lattice strain [12]. For a pure in-plane antiferrodistorsive octahedra rotation defined by the angle β (Figure 2), the in-plane lattice parameter is given by a non-linear relation to β:

$$a = \frac{d_{Pb-I}}{\sqrt{\left(\frac{1}{4}-u\right)^2+\left(\frac{1}{4}+u\right)^2}} \quad (1)$$

where u is the relative displacement of equatorial iodide atoms, which is also connected to the in-plane tilt angle $tan(\beta) = 4u$. For a square undistorted in-plane lattice, the angle β is equal to 180°. In many practical situations, the energetic cost of octahedra rotations is much smaller than the one of bond compression, in order to reduce the lattice constant. This is the case for the cubic to tetragonal structural phase transition of $CsPbI_3$ (Figure 2) [13].

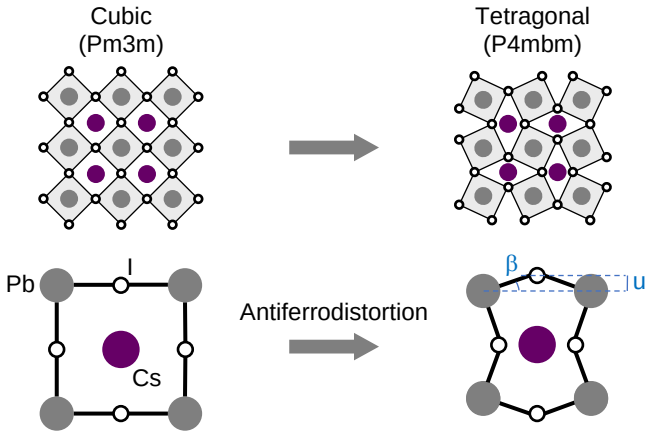

Figure 2. Structural phase transition of the 3D $CsPbI_3$ perovskite between the high temperature Pm3m cubic phase (T=645K) and the P4mbm tetragonal phase at low temperature (T=510K). Definition of the in-plane Pb-I-Pb β angle related to the antiferrodistorsive rotations of the perovskite octahedra in $CsPbI_3$.

2.3 Effect of lattice strain on the energetics

In solar cells as well as in LEDs, the energy level alignment between materials is crucial for charge extraction or injection and may be altered or improved by lattice strains. Thus, we investigated the effect of tensile and compressive strain on the electronic properties of perovskites. Under compressive strains, the absolute valence energy level E_V^{abs} gets less negative (lower absolute value) while the opposite occurs under tensile strains (more negative and higher absolute value). This effect is illustrated with density functional theory (DFT) based calculations performed on the cubic structure of $CsPbI_3$ under various degrees of both volumetric compressive and tensile strains (Figure 3). Calculations are performed using The effect is more pronounced at the valence band as compared to the conduction band. The variation can be understood from the type of the electronic coupling taking place at the valence band maximum (VBM) of these compounds. In fact, the VBM of these halide perovskites is made of an anti-bonding hybridization between I(5*p*) and Pb(6*s*) states. Under volumetric compressive strains, PbI bonds become shorter, which leads to more destabilized I(5*p*)- Pb(6*s*) coupling resulting in higher VBM level. The opposite effect happens under volumetric tensile strains in which Pb-I bonds get stretched leading to less destabilized I(5*p*)-Pb(6*s*) coupling and deeper VBM level. These strains ignore the effects of octahedral distortions/tilting which further influences the energy alignments. Our results indicate that given a perovskite composition and charge selective contact layers, one can fine-tune the energy level alignment of the device by subjecting the perovskite to strains. The latter could arise from the heterojunction between a 3D perovskite compound and a counterpart 2D structure or with the hole transporting layer (HTL) or electron transporting layer (ETL).

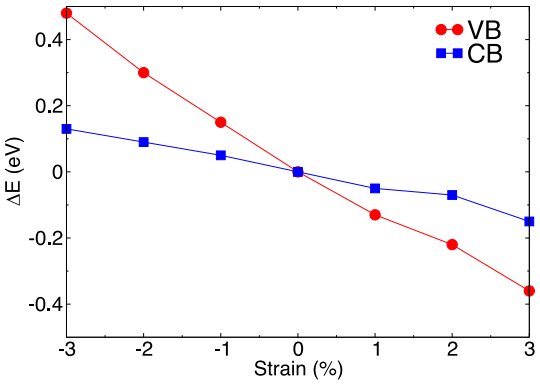

Figure 3. Variation of the valence band maximum (red) and conduction band minimum (blue) levels when a compressive (negative value) or tensile (positive value) strain is applied to the cubic structure of $CsPbI_3$. Levels computed on the equilibrium structure with no strain applied are taken as references.

2.4 Atomistic approaches for mixed cations halide perovskites

Perovskite compositions with mixed cations and/or anions raise the question on how to capture alloying and/or the dynamic and stochastic disorder of the organic cation beyond a few limited structural models. This holds for 3D bulk materials as well as for multi-layered perovskites or 2D/3D heterostructures. We explored various strategies because it turned out to be of dramatic importance to achieve reliable band alignments at temperatures relevant for device applications between two different perovskite materials as well as between a perovskite material and the HTL or ETL of interest. To this end, we developed and calibrated a dedicated method based on the use of pseudo-atoms that mimic mixed compositions (both for halides and Cs/FA mixtures).

We started to dig into a pseudo-atom approach, by inspecting cation alloying with the room-temperature pseudo-cubic $FAPbI_3$ and cubic CsPbI3 structures. The exploration of different computational strategies led us to opt for the most effective one, namely the FA molecule is replaced by a Cs atom in $FA^{PS}PbI3$ (FA^{PS}: FA replaced by Cs) while Cs is replaced by Na in $Cs^{PS}PbI3$ (Cs^{PS}: Cs replaced by Na). Figure 4 shows the variation of the lattice parameters of $FA^{PS}_xCs^{PS}_{1-x}PbI_3$ as a function of the mixing parameter x. We observe that Vegard's law for lattice constants is nicely recovered, which is the linear variation of the lattice constant with respect to the mixing parameter of the alloyed compound. In addition to the recovery of Vegard's law, our developed pseudo-atom approach allows to capture well experimental lattice mismatches between pseudo-3D and 2D compounds as shown in Table 1. This is important since the strains due to lattice mismatches may result in significant changes in the electronic structure of these ionic semiconductors (*vide supra*).

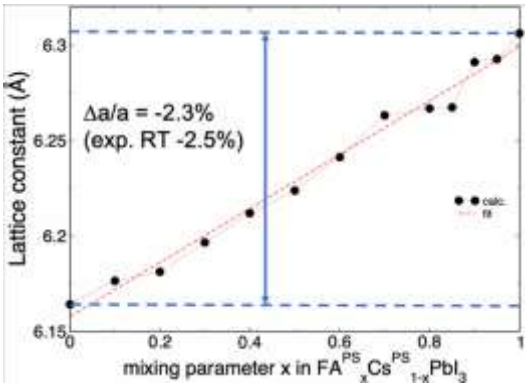

Figure 4. Variation of the DFT-optimized lattice constant of $FA^{PS}_xCs^{PS}_{1-x}PbI_3$ with respect to the mixing parameter x.

Table 1. Comparison of lattice constants between experimental and computed structures. The lattice mismatch between $FAPbI_3$ and the 2D compound is shown in parenthesis.

	Lattice constant (Å)	
Iodine based compounds	Experimental	Computed
		FA → FA^{PS}; Cs → Cs^{PS}
$FAPbI_3$ [a]	6.362	6.306
Pseudo-cubic $CsPbI_3$	6.201 (-2.5%)	6.164 (-2.3%)
BA_2PbI_4 [n]	6.212 (-2.4%)	6.134 (-2.7%)
PEA_2PbI_4 [n]	6.229 (-2.1%)	6.212 (-1.5%)
PA_2PbI_4 [b,n]	6.272 (-1.4%)	6.178 (-2.0%)

[a]Weller et al., J. Phys. Chem. Lett. 6, 3209 (2013); [b]PA=Pentylethylammonium; [n]The lattice constant of the 2D compound is obtained by taking its average in-plane lattice parameters divided by √2 (a_{2D}= <$a_{in\text{-}plane}$> /√2). The division by √2 is due to the cell doubling from cubic lattice to the 2D one.

Our modelling strategy thus allows to address few points: (i) getting rid of the issues of the dynamic disorder of FA in the cubic perovskite phase of $FAPbI_3$; (ii) fairly recovering the experimental mismatches between 2D and 3D compounds from the computationally relaxed structures; (iii) modelling cation alloying by mixing the contents of Cs^{PS} and FA^{PS} within the virtual crystal approximation (VCA); (iv) using this approach for large 2D/3D heterostructures, containing 3D alloys.

On the side of halide mixing, direct use of the VCA with optimized pseudopotentials of each halide specie was also implemented successfully (Figure 5). This strategy enables both for structural optimisation of alloys, including of complex heterostructures, and electronic structure calculations with a consistent computational protocol.

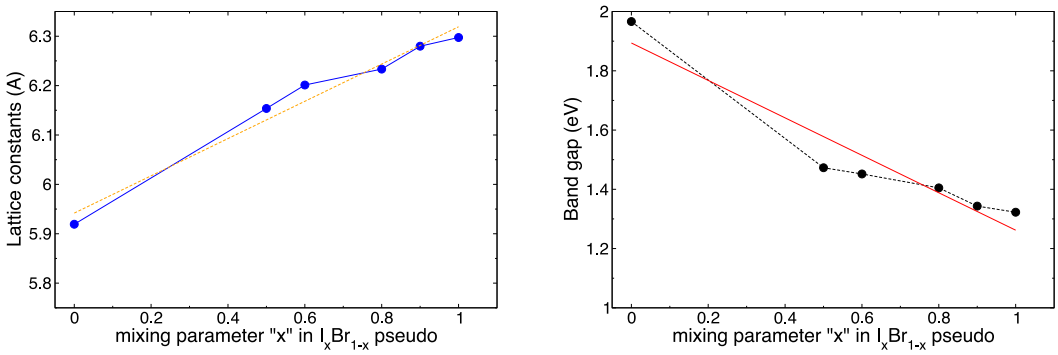

Figure 5. Computed variation of the lattice constant (left) and corresponding fundamental band gap (right panel) of $CsPb(I_xBr_{1-x})_3$ with respect to the mixing parameter x. Vegard's law is recovered.

2.5 Description of 2D/3D halide perovskite heterostructures

It was shown experimentally that the relation between in-plane and out-of-plane strain components strongly deviates in 2D/3D halide perovskite heterostructures from the $\varepsilon_{\perp} = \frac{-2C_{12}}{C_{11}}\varepsilon_{//}$ relation [7]. In order to obtain a proper description of the mechanical properties, a non-linear coupling between strain components sand octahedra tilt angle was introduced into a refined free energy expression. This 'improper flexoelastic' model [7] still deserves further experimental assessments. DFT studies of the lattice relaxation in model 2D/3D heterostructures tend to demonstrate that the strain shall be located at the interfaces between the interlayer and the perovskite layers. But due to the large sizes of the supercells (Figure 6), atomistic calculations remain challenging [17]. Additionally, the role of the large cations in the interlayer plays a capital role for the formation of such heterostructures. The mechanical flexibility of the interlayer is described by a set of empirical parameters in the 'improper flexoelastic' model [7], that influence the deviation from the classical relation between in-

plane and out-of-plane strain components and also the relaxation of the accumulated elastic energy in the perovskite layers due to lattice mismatch. Therefore, pure high members (n>5) have only being synthesized with moderate lattice mismatch and flexible cations such as BA in the interlayer [14], or by employing alternative cations leading to almost vanishing lattice mismatches [15]. Finally, the formation of complex halide perovskite heterostructures shall be ultimately limited by thermodynamic considerations, including the stability against the decomposition back into the initial precursors [16].

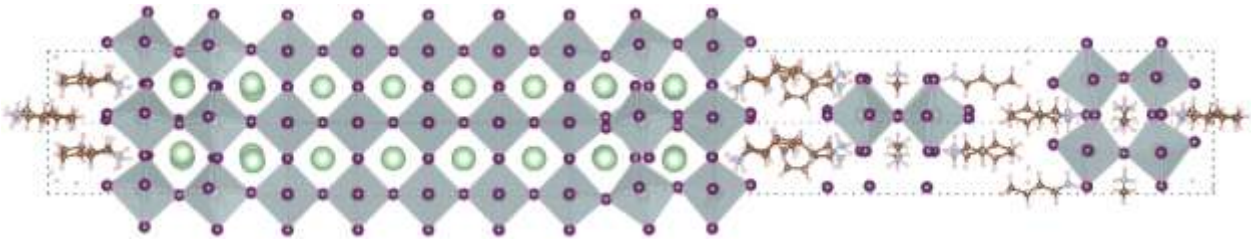

Figure 6. Structural model for the 2D/3D heterostructures. The bulk part is mimicked by a 9 octahedra thick layer that decompose in 5 central octahedra retaining the structural parameters of the optimized 3D bulk materials and on each side 2 octahedra which atomic positions are allowed to relax. One to two 2D layers are then adapted on each side with atomic positions allowed to relax. Whereas the in-plane parameters remain fixed to the 3D bulk value, the stacking axis is allowed to relax.

In order to go beyond mechanic models and perform atomistic calculations on such large systems, choices must be made looking for the best compromise between computational cost and accuracy. We start by taking advantage of the above-presented pseudo-atom approach for the description of 2D/3D heterostructures based on 3D $FAPbI_3$ and BA- or PEA-based 2D perovskites. The heterostructure is then built by interfacing slabs of 3D and 2D materials. While the 2D material present a natural way to build slabs because of its layered nature, the question is raised for 3D materials. We have retained a structural model made of layers containing 9 octahedra to represent the 3D bulk region as illustrated for the 2D/3D heterostructures shown in Figure 6. In a first attempt to model these complex heterostructures, the whole structure was allowed to relax, but this led in some cases either to numerical issues (calculations did not converge) or to unrealistic structures having large distortions [17]. Then we opt for an alternative strategy where the central five layers of the perovskite section remain frozen to better mimic the 3D bulk region, thus imposing fixed in-plane lattice parameters. This is especially realistic for 2D/3D perovskite heterostructures since a thick 3D layer will impose its in-plane lattice parameter to the 2D layers further deposited on top of it. When building interfaces with HTL or ETL, the 3D perovskite layer may adapt on the substrate (e.g. for NiO_x) depending on the elastic properties of each material.

We have used those models for heterostructures based on $FAPbI_3$ and the thinnest (n=1) 2D materials BA_2PbI_4 and PEA_2PbI_4 (Figure 7). First, the sizeable lattice mismatch predicted based on the experimental database was confirmed by first-principle structural optimization of the bulk 2D and 3D perovskites. We then constructed heterostructures, considering different surface terminations of the 3D section and we consider the resulting band alignments for each case. Figure 7 shows the 2D/3D heterostructures and the evolution of band alignment when going from one to two 2D layers sandwiched between the 3D stack. Comparable band alignments are predicted for $FA^{PS}PbI_3/BA_2PbI_4$ and $FA^{PS}PbI_3/PEA_2PbI_4$. Considering also experimental data, we conclude that the band offsets prevent efficient carrier extraction from the 3D

region to the 2D region. Therefore, further modification to overcome the barrier is needed, such as use of ultrathin passivation 2D layers to allow tunnelling through the 2D region.

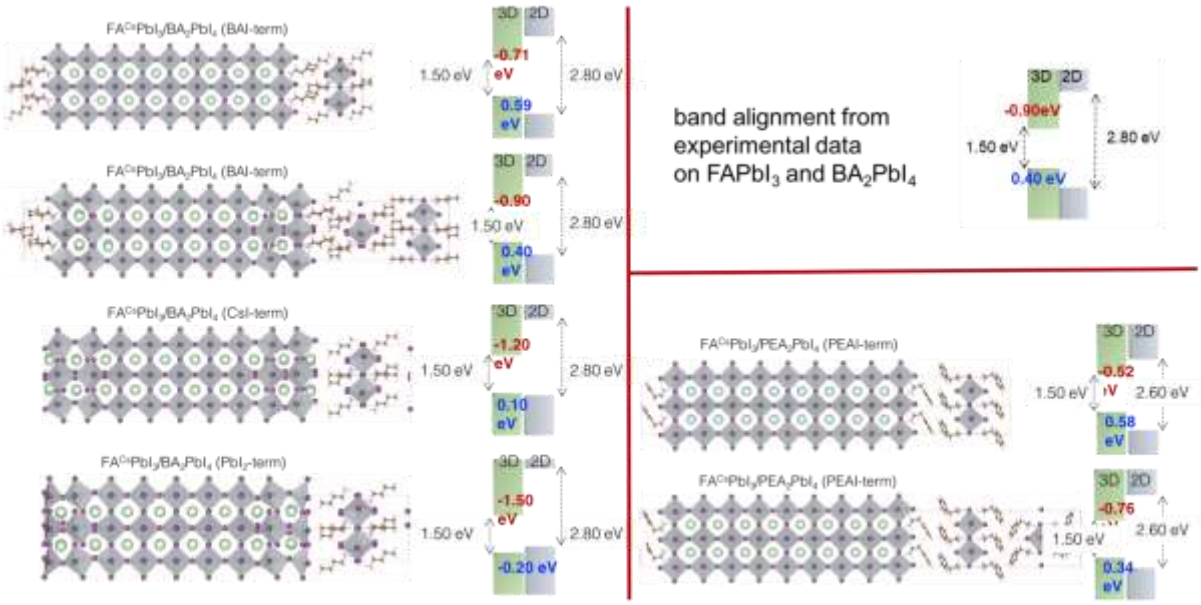

Figure 7. The atomistic models for $FA^{PS}PbI_3/BA_2PbI_4$ (left) and $FA^{PS}PbI_3/PEA_2PbI_4$ (bottom right) heterostructures, considering one and two layers for 2D perovskite on top of the 3D with specific surface termination indicated in parentheses. The predicted band offsets are computed from DFT while experimental continuum band gaps have been used to align the bottom of the conduction bands. Band alignment based on experimental data is shown in the top right panel.

We expect the band alignment to be more favorable for charge carrier extraction when considering thicker 2D perovskites (n>1) on top of the 3D. We investigate energy level alignment based on these complex heterostructures (Figure 8). We predict almost flat valence energy alignment between the 2D and 3D materials for extraction of holes for larger n-values starting from n=4. Even for larger values, the barrier for electrons is anticipated to remain sizeable.

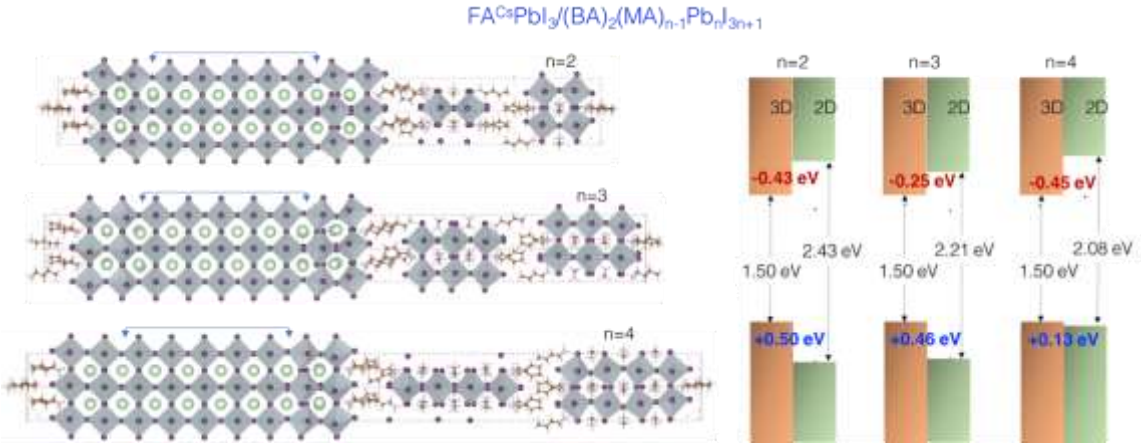

Figure 8. Atomistic models for $FA^{PS}PbI_3/BA_2MA_{n-1}Pb_nI_{3n+1}$ (n=2-4, left) and corresponding predicted band alignments (right). The predicted band offsets are computed from DFT while experimental continuum band gaps have been used to align the bottom of the conduction bands.

3. CONCLUSIONS

2D/3D halide perovskites are attractive solutions to build stable perovskite solar cell architectures, while preserving the impressive efficiencies of the state-of-the-art 3D perovskite cells. Here, we proposed a set of technical tricks that will be useful to computational material scientists willing to describe at the atomic level such complex heterostructures. Based on chemical and physical intuitions, it shall help researchers to make educated guess in selecting materials and ligands to optimize future optoelectronic devices. In particular, we establish that better performances are expected by using 2D perovskites with large n values. The limitation of strain accumulation in the heterostructure is a prerequisite than can be afforded by proper chemical and structural engineering.

REFERENCES

[1] Byranvand, M. M., Otero-Martínez, C., Ye, J., Zuo, W., Manna, L., Saliba, M., Hoye, R. L. Z., Polavarapu, L., "Recent Progress in Mixed A-Site Cation Halide Perovskite Thin-Films and Nanocrystals for Solar Cells and Light-Emitting Diodes." Adv. Opt. Mater. 10, 2200423 (2022).

[2] Tsai, H., Nie, W., Blancon, J.-C., Stoumpos, C.C., Soe, C. M. M., Yoo, J., Crochet, J., Tretiak, S., Even, J., Sadhanala, A., Azzellino, G., Brenes, R., Ajayan, P. M., Bulović, V., Stranks, S. D., Friend, R. H., Kanatzidis, M. G. and Mohite, A. D., "Stable light-emitting diodes using phase-pure Ruddlesden–Popper layered perovskites. " Adv. Mat. 30, 1704217 (2018).

[3] Sidhik, S., Wang, Y., De Siena, M., Asadpour, R., Torma, A. J., Terlier, T., Ho, K., Li, W., Puthirath, A. B., Shuai, X., Agrawal, A., Traore, B., Jones, M., Giridharagopal, R., Ajayan, P. M., Strzalka, J., Ginger, D. S., Katan, C., Alam, M. A., Even, J., Kanatzidis, M. G. and Mohite, A. D., "Deterministic fabrication of 3D/2D perovskite bilayer stacks for durable and efficient solar cells." Science 377, 1425–1430 (2022).

[4] Azmi, R., Ugur, E., Seitkhan, A., Aljamaan, F., Subbiah, A. S., Liu, J., Harrison, G. T., Nugraha, M. I., Eswaran, M. K., Babics, M., Chen, Y., Xu, F., Allen, T. G., Rehman, A. u., Wang, C.-L., Anthopoulos, T. D., Schwingenschlögl, U., De Bastiani, M., Aydin, E. & De Wolf, S., "Damp heat–stable perovskite solar cells with tailored-dimensionality 2D/3D heterojunctions." Science 376, 73–77 (2022).

[5] Wang, Z., Lin, Q., Chmiel, F. P., Sakai, N., Herz, L. M. & Snaith, H. J., "Efficient ambient-air-stable solar cells with 2D–3D heterostructured butylammonium-caesium-formamidinium lead halide perovskites." Nat. Energy 2, 17135 (2017).

[6] Li, W., Sidhik, S., Traore, B., Asadpour, R., Hou, J., Zhang, H., Fehr, A., Essman, J., Wang, Y., Hoffman, J. M., Spanopoulos, I., Crochet, J. J., Tsai, E., Strzalka, J., Katan, C., Alam, M. A., Kanatzidis, M. G., Even, J., Blancon, J.-C. & Mohite, A. D., "Light-activated interlayer contraction in two-dimensional perovskites for high-efficiency solar cells." Nat. Nanotechnol. 17, 45–52 (2022).

[7] Kepenekian, M., Traore, B., Blancon, J.-C., Pedesseau, L., Tsai, H., Nie, W., Stoumpos, C. C., Kanatzidis, M. G., Even, J., Mohite, A. D., Tretiak, S. and Katan, C., "Concept of lattice mismatch and emergence of surface states in two-dimensional hybrid perovskite quantum wells," Nano Lett. 8, 5603−5609 (2018).

[8] Cornet, C., Schliwa, A., Even, J., Doré, F., Celebi, C., Létoublon, A., Macé, E., Paranthoën, C., Simon, A., Koenraad, P. M., Bertru, N., Bimberg, D. and Loualiche, S., "Electronic and optical properties of InAs/InP quantum dots on InP(100) and InP (311)B substrates: Theory and experiment," Phys. Rev. B 121, 085502 (2018).

[9] Ferreira, A. C., Létoublon, A., Paofai, S. Raymond, S., Ecolivet, C., Rufflé, B., Cordier, S., Katan, C., Saidaminov, M. I., Zhumekenov, A. A., Bakr, O. M., Even, J. and P. Bourges, "Elastic Softness of Hybrid Lead Halide Perovskites," Phys. Rev. Lett. 121, 085502 (2018).

[10] Katan, C., Mohite, A.D. and Even, J., "Entropy in halide perovskites," Nature Mat. 17, 377–384 (2018).

[11] Tamarat, P., Prin, E., Berezovska, Y., Moskalenko, A., Nguyen, T. P. T., Xia, C., Hou, L., Trebbia, J.-B., Zacharias, M., Pedesseau, L., Katan, C., Bodnarchuk, M. I., Kovalenko, M. V., Even, J. and Lounis, B., "Universal scaling laws for charge-carrier interactions with quantum confinement in lead-halide perovskites," Nat. Commun. 14, 229 (2023).

[12] Pedesseau, L., Sapori, D., Traore, B., Robles, R., Fang, H.-H., Loi, M. A., Tsai, H., Nie, W., Blancon, J.-C., Neukirch, A., Tretiak, S., Mohite, A. D., Katan, C., Even, J. and Kepenekian, M., "Advances and Promises of Layered Halide Hybrid Perovskite Semiconductors," ACS Nano 10, 9776−9786 (2016).

[13] Marronnier, A., Roma, G., Boyer-Richard, S., Pedesseau, L., Jancu, J. M., Bonnassieux, Y., Katan, C., Stoumpos, C. C., Kanatzidis, M. G. and Even, J., "Anharmonicity and disorder in the black phases of cesium lead iodide used for stable inorganic perovskite solar cells," ACS Nano 12, 3477−3486 (2018).

[14] Stoumpos, C.C., Soe, C. M. M., Tsai, H., Nie, W., Blancon, J.-C., Cao, D.H., Liu, F., Traoré, B., Katan, C., Even, J., Mohite, A.D. and Kanatzidis, M.G., "High members of the 2D Ruddlesden-Popper halide perovskites: synthesis, optical properties, and solar cells of $(CH_3(CH_2)_3NH_3)_2(CH_3NH_3)_4Pb_5I_{16}$," Chem 2, 427-440 (2018).

[15] Mao, L., Kennard, R. M., Traore, B., Ke, W., Katan, C., Even, J., Chabinyc, M. L., Stoumpos, C. C. and Kanatzidis, M.G., "Seven-layered 2D hybrid lead iodide perovskites," Chem 5, 2593-2604 (2019).

[16] Soe, C.M M., Nagabhushana, G. P., Shivaramaiah, R., Tsai, H., Nie, W., Blancon, J.-C., Melkonyan, F., Cao, D.H., Traoré, B., Pedesseau, L., Kepenekian, M., Katan, C., Even, J., Marks, T. J., Navrotsky, A., Mohite, A. D., Stoumpos, C. C. and Kanatzidis, M.G., "Seven-layered 2D hybrid lead iodide perovskites," PNAS 116, 58-66 (2019).

[17] Traore, B., Basera, P., Ramadan, A.J., Snaith, H. J., Katan, C. and Even, J., "A theoretical framework for microscopic surface and interface dipoles, work functions, and valence band alignments in 2D and 3D halide perovskite heterostructures," ACS Ener. Lett., 7, 349−357 (2022).